Ultrasonics Sonochemistry 28 (2016) 150–160

Contents lists available at ScienceDirect

Ultrasonics Sonochemistry

journal homepage: www.elsevier.com/locate/ultson

Investigation of TiO_2 photocatalyst performance for decolorization in the presence of hydrodynamic cavitation as hybrid AOP

Bhaskar Bethi [a], S.H. Sonawane [a,*], G.S. Rohit [a], C.R. Holkar [b], D.V. Pinjari [b], B.A. Bhanvase [c], A.B. Pandit [b]

[a] Department of Chemical Engineering, National Institute of Technology, Warangal 506004, Telangana State, India
[b] Chemical Engineering Department, Institute of Chemical Technology, Matunga, Mumbai, MS, India
[c] Chemical Engineering Department, Laxminarayan Institute of Technology, RTM Nagpur University, Nagpur 440033, MS, India

ARTICLE INFO

Article history:
Received 3 April 2015
Received in revised form 9 July 2015
Accepted 9 July 2015
Available online 10 July 2015

Keywords:
Sonochemical synthesis
Nanophotocatalyst
Hydrodynamic cavitation
Hybrid advanced oxidation process
Waste water treatment

ABSTRACT

In this article, an acoustic cavitation engineered novel approach for the synthesis of TiO_2, cerium and Fe doped TiO_2 nanophotocatalysts is reported. The prepared TiO_2, cerium and Fe doped TiO_2 nanophotocatalysts were characterized by XRD and TEM analysis to evaluate its structure and morphology. Photo catalytic performance of undoped TiO_2 catalyst was investigated for the decolorization of crystal violet dye in aqueous solution at pH of 6.5 in the presence of hydro dynamic cavitation. Effect of catalyst doping with Fe and Ce was also studied for the decolorization of crystal violet dye. The results shows that, 0.8% of Fe-doped TiO_2 exhibits maximum photocatalytic activity in the decolorization study of crystal violet dye due to the presence of Fe in the TiO_2 and it may acts as a fenton reagent. Kinetic studies have also been reported for the hybrid AOP (HAOP) that followed the pseudo first-order reaction kinetics.

© 2015 Elsevier B.V. All rights reserved.

1. Introduction

Dyes are having many applications in different industrial processes such as textile, printing, leather, paint, plastic, food, cosmetics, and pharmaceutical industries [1]. Waste water discharge from these industries containing high concentrations of dyes, high toxicity and intense color causes serious problems on surrounding ecosystem [2]. Many treatment methods are available for the treatment of above mentioned industrial wastewater, such as conventional biological treatment (aerobic and anaerobic), adsorption, coagulation and flocculation. The main drawbacks of these methods are not being able to completely degrade the dye molecules present in the waste water due to the complex and bio recalcitrant nature of the dye molecules. Azo dyes are known to as more non-biodegradable under aerobic biological conditions and these dyes are converted to more hazardous intermediates under anaerobic conditions [3]. Some methods such as coagulation/flocculation and adsorption are physical treatment methods and these methods did not involve chemical transformation and therefore generally transport the waste components from one phase to another phase, that leads to secondary waste pollutant on the environment [4,5]. Therefore, it is necessary to find an effective treatment technology for the degradation of the complex and non-biodegradable molecules to smaller molecules. For this application, advanced oxidation processes (AOPs) have been employed and evaluated since the 20th century to degrade azo dyes from the wastewater. Among AOPs, electrolysis and photo catalysis are extensively studied [6]. AOPs involve the generation of hydroxyl radicals and complete oxidization of such pollutants including dyes converted into end products, such as CO_2, H_2O, etc. [7]. Recent literature has indicated that hybridization of different AOPs has been found to be more efficient for the wastewater treatment than individual oxidation process [8,9].

Recently, hydrodynamic and acoustic cavitation has been widely applied as an advanced oxidation technology along with other AOPs for wastewater treatment as a hybrid treatment technique [10–12]. When an aqueous solution is passed through a mechanical constriction, large pressure differentials are generated due to the change in flow geometry. If the pressure of the aqueous solution at the constriction falls below the vapor pressure of the aqueous solution, cavities are formed, and grow and/or subsequently collapse on the recovery of pressure [13]. Sudden collapse of these cavities (occurring in microseconds) yields localized high temperatures and pressures. Water molecules under such extreme conditions undergo thermal dissociation to form hydroxyl radicals, which are powerful oxidants for the complete mineralization of many organic pollutants [14].

* Corresponding author.
E-mail address: shirishsonawane09@gmail.com (S.H. Sonawane).

http://dx.doi.org/10.1016/j.ultsonch.2015.07.008
1350-4177/© 2015 Elsevier B.V. All rights reserved.

Researchers have studied photocatalysis extensively among other AOPs as a wastewater treatment method using nano sized and micro sized photocatalysts with doping and/or in pure state.

Among many photocatalysts TiO_2 has been widely studied because of its chemical inertness, strong oxidizing power, and long-term stability against photo and chemical corrosion, suitable band gap energy and electronic and optical properties [15–18]. The main drawbacks which are associated with the use of TiO_2 in waste water treatment are undesirable recombination of electrons and holes, and low efficiency under irradiation in the visible region [20,21]. Scientists are overcome this problem by extending the light absorption range of TiO_2 from UV to visible light and to improve the photocatalytic activity of TiO_2 [22]. Dopants, such as transitional metals can be loaded on to TiO_2 to minimize the recombination of photo-generated electrons and photo-generated holes and also shifts the excitation wavelength from the UV to the visible light spectrum [19–24]. In the past the researchers are used the transition metals (Fe, Al, Ni, Cr, Co, W, V and Zr), metal oxides (Fe_2O_3, Cr_2O_3, CoO_2, MgO + CaO and SiO_2), transition metal ceramics (WO_3, MoO_3, Nb_2O_5, SnO_2 and ZnO) and anionic compounds (C, N, and S) to dope TiO_2 to improve its applicability [25–28]. In the literature very few articles are reported the work on Ce doped TiO_2 catalysts. They reported that the effect of Ce doped TiO_2 catalysts are strongly depends on the various factors, such as the synthesis method and the cerium content [21,29,30]. In this work, the reason for choosing dopants, such as transitional metals was to improve its catalytic activity and to reduce the recombination of photo-generated electrons and photo-generated holes. Rauf [22] has given an overview on the photocatalytic degradation of azo dyes in the presence of TiO_2 doped with selective transition metals. Higher catalytic activity has been reported for the Ce doped TiO_2 materials for photo-degradation of dyes and other pollutants. Cerium oxides have attracted much attention due to the optical and catalytic properties associated with the redox pair of Ce^{3+}/Ce^{4+}. Cerium extends the photo response into the visible region, this can lead to an increase in the charge separation efficiency of surface electron–hole pairs. Earlier there are many reports of Fe doping on TiO_2 to improve its photo catalytic activity among a variety of transitional metals and also Fe on TiO_2 acts as a Fenton reagent (Fe^{2+}) has shown the better degradation performance of organic pollutants than other transition metals. Shirsath et al. [31] synthesized the titanium dioxide nanoparticles doped with Fe and Ce using sonochemical approach. They found that Ce doped TiO_2 exhibits maximum photocatalytic activity followed by Fe-doped TiO_2 and the least activity was for only TiO_2 for the degradation of crystal violet (CV) dye. Narayana et al. [32] have synthesized the pure TiO_2, Fe and Co doped photocatalysts via sol–gel method. From the malachite green decolorization study, they observed that Fe-doped TiO_2 showed highest photocatalytic activity among the other two photocatalysts with 98% decolorization in 2 h. Ramirez et al. [33] have studied the photocatalytic degradation of acid orange 7 (AO7) using Ce-doped TiO_2 slurry and employing solar irradiation. They have observed that AO7 has shown higher decolorization when Ce content in the TiO_2 is about 1.0% (by weight) compared to TiO_2. There is effect of synthesis method on TiO_2 structures and hence on photocatalytic activity. Anatase and rutile are two major phases are present in TiO_2. Composition of these phases varies from 20% to 80%. The anatase phase shows better degradation capability compared to rutile phase of TiO_2. Particle size, surface area, and their calcinations temperature will also adversely affect on the photocatalytic activity of TiO_2. Andronic et al. [34] reported the synthesis of TiO_2 by sol–gel method, the resultant TiO_2 powder having 40% anatase and 60% rutile was shown the degradation of methyl orange up to 37% in 30 min of UV irradiation. Samira et al. [35] reported the crystal violet degradation of initial concentration: 5×10^{-5} mol/L, using nanoanatase TiO2 having anatase and rutile phases in the ratio of 3:1 was shown the degradation rate greater than 99.5% on UV illumination for 45 min. It was also confirmed in the recent literature that ultrasound assisted synthesis of TiO_2 has shown the better decolorization performance than the conventional synthesis technique [31]. The ultrasound assisted synthesis technique able to produce the very small size (nanometer range) TiO_2 particles having more specific surface area which is able to adsorb the large quantity of dye molecules on active sites of the catalyst leads to better decolorization.

Some of the articles have reported the wastewater treatment technique based on photocatalysis combined with cavitation technique as hybrid AOP. Very few articles were found on HC/UV and HC/UV/TiO_2 combination, for dyes decolorization and other organic pollutants (pesticides, pharmaceutical compounds). Though literature reports are found on US/UV/TiO_2 combination, but scale up of waste water treatment using ultrasound cavitation is not effective solution [30]. It requires more energy compared to hydrodynamic cavitation. It can possible to scale up the waste water treatment using HC due to the production of more cavitation yield, less cost of operation, cheap design. It was confirmed that HC is potentially suitable for scale up issues in waste water treatment based on cavitation. Kalumuck [36] reported the degradation of p-nitrophenol in wastewater using hydrodynamic cavitation in a re-circulatory pipe flow. It has been reported that the hydrodynamic cavitation has shown about 20 times more rate of degradation compared to the ultrasonic horn and the oxidation efficiency is almost 25 times more for the hydrodynamic cavitating jets. Sivakumar and Pandit [37] studied the applicability of hydrodynamic cavitation for the degradation of Rhodamine B dye solution, they reported that hydrodynamic cavitation was much more energy efficient compared to acoustic cavitation. Hydrodynamic cavitation unit using multiple hole orifice plates has been reported to give cavitational yields (extent of degradation per unit energy supplied), which are two times higher than the best acoustic cavitation device.

Wang et al. [38] have studied the decolorization of an azo dye, C.I. reactive red 2 (RR2) using TiO_2 photocatalysis coupled with water jet cavitation. Bagal et al. [39] have studied the degradation of diclofenac a pharmaceutical drug in wastewater samples using a combined approach of hydrodynamic cavitation and heterogeneous photocatalysis. They found that the degradation of diclofenac is about 95% with 76% reduction in TOC value. Although there are many studies reported in the literature on doped TiO_2 with Fe and Ce as a photocatalysts for the degradation of various dyes, none of the studies to the best of our knowledge, have been reported in the literature on combination of hydrodynamic cavitation and doped photocatalysis. The novelty of this research is to study the doped TiO_2 photocatalysts with the combination of hydrodynamic cavitation for the treatment of dye waste water to know the effect of doped photocatalyst.

The present work reports the ultrasonic assisted synthesis of TiO_2, Fe-doped TiO_2, Ce-doped TiO_2 nanophotocatalysts. Prepared photo catalysts have been used for the degradation of crystal violet (CV) dye in the presence of hydrodynamic cavitation combined with photo catalysis.

2. Materials and methods

2.1. Materials

For the synthesis of pure TiO_2, Fe–TiO_2, and Ce–TiO_2, chemicals namely Titanium Tetra isopropoxide (TTIP) were obtained from Spectrochem Pvt. Ltd. Mumbai, India. Cerium nitrate and ferric nitrate were obtained from S.D. Fine Chemicals Ltd., Mumbai, India. Sodium hydroxide, methanol and acetone were procured

from Molychem Ltd., Mumbai, India. For the decolorization study, crystal violet dye ($C_{25}N_3H_{30}Cl$) was procured from Sisco Research Laboratories Pvt. Ltd. Mumbai, India. All the chemicals procured were of analytical grade and were used as obtained from the supplier.

2.2. Experimental setup

The experimental setup of hydrodynamic cavitation coupled with photocatalytic reactor is shown in Fig. 1. This set up includes a tank of 5 L volume along with UV light assembly inside the tank. The setup is arranged in a closed loop manner, which includes a feed tank, positive displacement pump (power = 1.1 kW), pressure gauges and valves. Cooling jacket is provided to the feed tank in order to control temperature. Suction side of the pump is connected to the bottom side of the feed tank and the discharge line from the pump branches into two lines. The main line consists of a circular venturi and second line is the bypass line. In the present study, circular venturi with 2 mm throat diameter is used as a cavitating device. Geometrical dimensions of circular venturi are shown in Fig. 2. A bypass line is provided to control the flow through the main lines. Control valves and pressure gauges are provided at appropriate places to control the flow rate through the lines containing the cavitating device (venturi) and to measure the fluid pressures respectively. Alternatively, variable frequency drive (VFD) is also provided to control the motor rpm such that the flow through the main line can be controlled directly by changing the number of piston stroke per minute of the positive displacement pump, while keeping bypass line closed. The material of construction of the entire system except cavitating device is stainless steel (SS-316), whereas cavitating device, circular venturi is made up of brass. Portable assembly, made up of quartz, containing high pressure mercury vapor lamp (125 W) with cooling jacket, is placed centrally in the feed tank for the UV–visible irradiation.

2.3. Analytical procedure

The crystal violet dye samples were collected for every interval and analyzed using UV–Vis Spectrophotometer to observe a change in the absorbance value of crystal violet dye with respect to time at a maximum wavelength (λ_{max}) of 590 nm. The concentration of crystal violet dye was then calculated using the calibration curve prepared for crystal violet dye.

2.4. Synthesis of pure TiO_2 and doped TiO_2 nanophotocatalysts

In a typical synthesis procedure, sonochemical technique [31,40] was used to prepare the pure TiO_2 nanophotocatalyst. The synthesis procedure begins with 10 mL of titanium isopropoxide (TTIP) mixed with 2 mL acetone and 2 mL methanol in a 250 mL beaker (ultrasound reactor). The reactor was placed in a constant temperature bath and the sonication was carried in the presence of ultrasonic irradiation using an ultrasonic horn (Dakshin ultrasonic probe sonicator, 22 kHz operating frequency, 130 W power supply). 50 mL sodium hydroxide solution was added drop wise into the ultrasound reactor. During the addition of sodium hydroxide solution to the above mixture, a white precipitate was formed. After the addition of 50 mL of sodium hydroxide solution, the mixture was further sonicated for 30 min. After 30 min of irradiation the solution was kept undisturbed for settling of the precipitate. The resulting precipitate was filtered, dried and calcined at 200 °C for 2 h.

Procedure used for the synthesis of pure TiO_2 [31,40] has been used for the synthesis of Fe-doped TiO_2, and Ce-doped TiO_2, including the addition of ferric nitrate and cerium nitrate carried out individually for the synthesis of Fe doped TiO_2 and Ce-doped TiO_2 nanophotocatalyst with molar ratios of 0.8 and 1.6 (mol%) of Fe to TiO_2 and Ce to TiO_2 respectively. Schematic experimental setup for the synthesis of undoped and doped TiO_2 nanoparticles is shown in the Fig. 3. Typical method for the synthesis of Fe–TiO_2 and Ce–TiO_2 is shown in the Fig. 4. The same method was adopted for the synthesis of Ce–TiO_2 except the addition of ferric nitrate, in the place of ferric nitrate; cerium nitrate was added to synthesize Ce–TiO_2 nanophotocatalyst.

2.5. Characterization

Pure TiO_2, Fe–TiO_2, Ce–TiO_2 nanophotocatalysts prepared through acoustic cavitation technique was characterized by using powder X-ray diffractometer (Phillips PW 1800, range is 6–80°

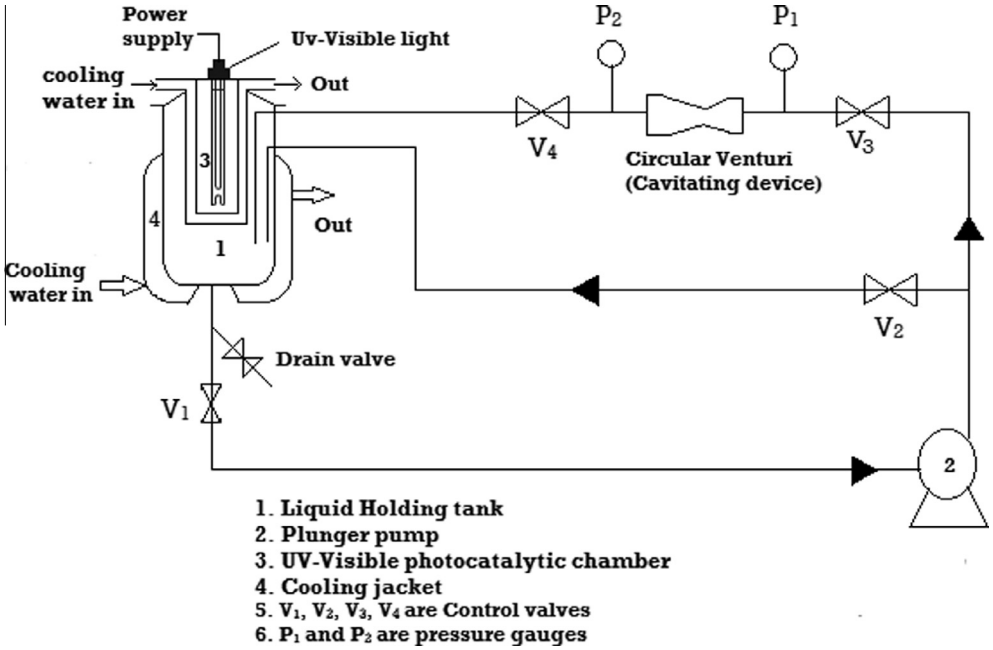

Fig. 1. Hydrodynamic cavitation set up with UV–Vis photocatalysis system.

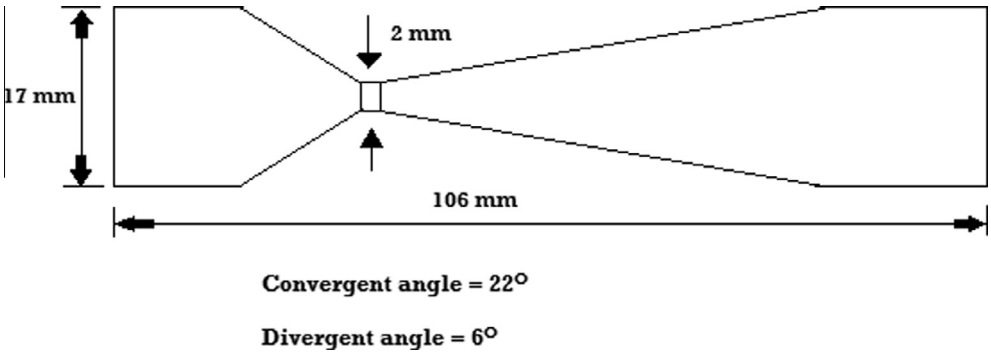

Fig. 2. Geometrical dimensions of cavitating device (circular venturi).

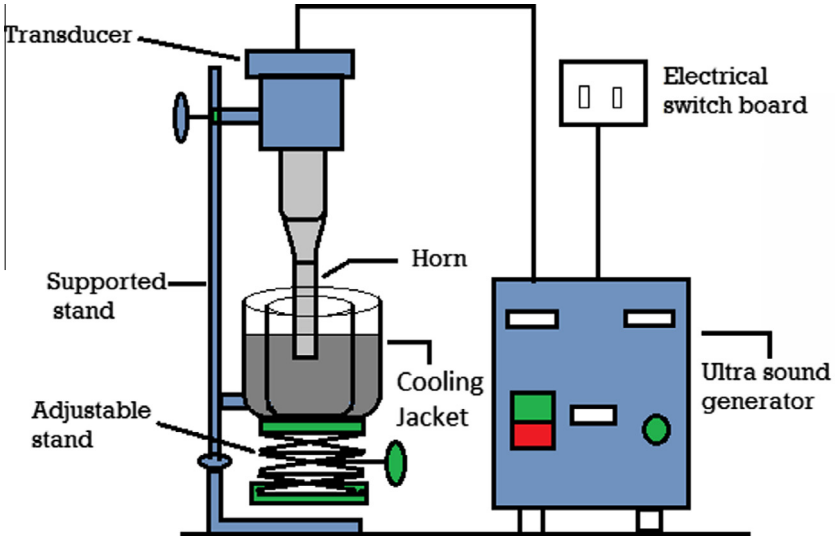

Fig. 3. Experimental setup for synthesis of undoped and doped TiO_2 nanoparticles.

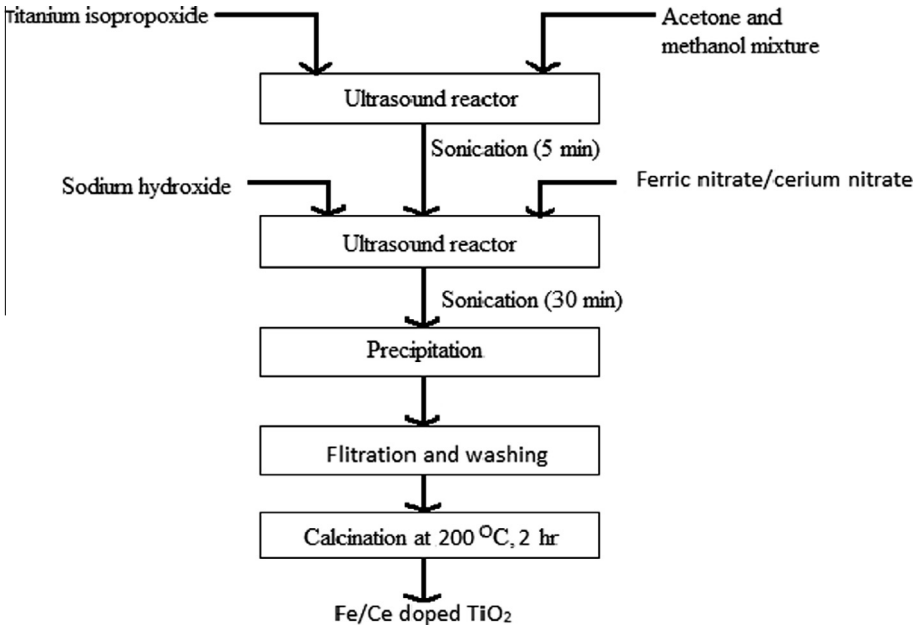

Fig. 4. Method for synthesis of Fe–TiO_2.

2θ). The morphology and particle size of these three photocatalysts were characterized by transmission electron microscopy (TEM, H-7650 accelerating voltage of 120 kV).

3. Results and discussion

3.1. XRD analysis of doped and undoped TiO_2 nanoparticles prepared by sonochemical method

Powder X-ray diffraction (XRD) was used for identification of the particles size, crystal structures. TiO_2 powder prepared by sonochemical approach and calcined at 200 °C was used in X-ray powder diffraction (XRD) analysis to characterize the particles structure and crystal size. XRD pattern of ultrasonically prepared TiO_2 powder samples is shown in the Fig. 5. As observed from the XRD pattern of TiO_2, the peaks are generated at $2\theta = 27.5°$, 30°, 42°, 48°, 54°, 62° and 72° confirms the TiO_2 powder was predominantly crystalline in nature with anatase as a major phase. Among the other peaks in XRD pattern of TiO_2, the initial peaks which are generated between the 2θ range of 25⁻30° such as 27.5° and 30° are the prominent peaks with high intensity, which is used to determine crystallite size. These high intensity peaks indicated that the crystalline phase of anatase TiO_2 was successfully formed.

The XRD patterns of 0.8% Fe-doped TiO_2 powder prepared by sononochemical approach and calcined at 200 °C showed the main peaks at $2\theta = 25.8°$, 36.9°, 48.1°, 54.1° and 62.4°. These peaks are corresponding to the anatase crystalline phase (which is photocatalytically active). The XRD pattern of Fe–TiO_2 also showed the peak at 34.4°, the peak which is generated at this angle was assigned to the presence of Fe in hematite form in TiO_2 [41,26]. Similarly the XRD patterns of Ce-doped TiO_2 for 0.8% Fe–TiO_2 showed the generation of main peaks at $2\theta = 30°$, 37.4°, 47.8°, 54.5° and 62.7° again related to the anatase crystalline phase.

It is also observed that the XRD patterns of Ce doped TiO_2 showed the presence of good intensity peaks at 30° and 30.6°. These peaks intensity are assigned to cerium titanate – $Ce_xTi_{1-x}O_2$ [21,42]. Thus, one can observe in the case of XRD pattern of ultrasonically prepared Ce doped TiO_2 consists of peak at $2\theta = 30°$, this peak corresponding to the presence of cerium as a separate cubic CeO_2, or as cerium titanate in the TiO_2 phase [31].

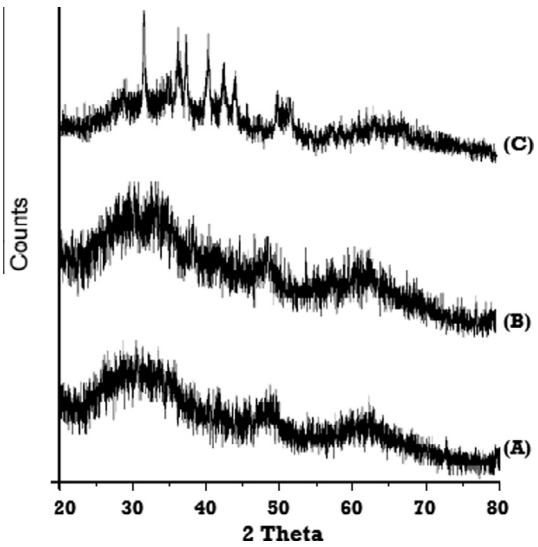

Fig. 5. XRD pattern of Ce-doped TiO_2, Fe-doped TiO_2 and undoped TiO_2 powder prepared by sonochemical method [(A) TiO_2, (B) Fe–TiO_2, (C) Ce–TiO_2].

From the XRD patterns of pure TiO_2, Fe–TiO_2 and Ce–TiO_2, the crystallite sizes of the synthesized TiO_2, Fe–TiO_2 and Ce–TiO_2 nanoparticles were estimated using Scherrer equation [43]:

$$d = \frac{k\lambda}{\beta\cos\theta} \quad (1)$$

where

'd' is crystallite size in nanometer,
'k' is shape factor constant, which is 0.89,
'β' is the full width at half maximum (FWHM) in radian,
'λ' is the wave length of the X-ray which is 1.540598 nm for Cu target Kα radiation and
'θ' is the Bragg diffraction angle.

By using the above data the estimated crystalline sizes for pure TiO_2, Fe–TiO_2 and Ce–TiO_2 are shown in Table 1. In detail, the initial observed peak at $2\theta = 27.5°$, 27.8° and 26.5° for TiO_2, Fe–TiO_2, and Ce–TiO_2 respectively and the full width of maximum intensity for all three photocatalysts are 0.016711.

3.2. TEM analysis and particle size distribution of TiO_2 and doped TiO_2 nanoparticles

Transmission electron microscope (TEM) was used to study the crystal structure, morphology, shapes and particle size. Figs. 6–8 shows the typical transmission electron microscopic images of TiO_2, 1.6 mol% of Fe–TiO_2 and 1.6 mol% of Ce–TiO_2 calcined at 200 °C for 2 h. TEM images indicates that the particles of TiO_2, Fe-doped TiO_2, and Ce–TiO_2 are relatively uniform and are very small in size (<100 nm). It could be clearly interpreted that, the crystal growth formation has not occurred in the three photocatalysts synthesized in this work and shows uniform doping of Fe and Ce on TiO_2. The main reason for the desegregation of crystals is due to the presence of ultrasonic irradiation while synthesis of photocatalysts. During the ultrasonic irradiation, number of micro jets are formed due to the cavitational activity [31], these micro jets avoid the interaction between crystals which are formed during synthesis and also breakdown the crystals into smaller size. This phenomenon helps to reduce the agglomeration of particles hence the smaller and more uniform particles size and uniform shape could be observed.

One can observe from the studies of TEM on pure TiO_2, Fe–TiO_2 and Ce–TiO_2 prepared by various synthesis techniques reported in the literature, tells that all the techniques other than ultrasonic assisted synthesis result into the generation of enormous agglomerated crystalline phase, non-uniform and large crystalline sizes.

3.3. Decolorization of CV through HC alone

In a typical experimental procedure, 50 mg/L of crystal violet (CV) dye were used for the preparation of 5 L crystal violet dye stock solution. The following operating conditions such as constant temperature (35 °C), constant pressure (5 kg/cm^2 pump discharge pressure to the cavitating device) and normal solution pH 6.5 were used for the study of CV degradation. In this study, experiments were carried out at pH of 6.5, which is the solution pH of the crystal violet dye. A reason for keeping constant pH is reported as follows.

Table 1
Estimated crystalline sizes of photocatalysts prepared by sonochemical method.

Type of photocatalyst	2θ	β	Particles size (nm)
Pure TiO_2	27.5	0.016711	84.47
Fe-TiO_2	27.8	0.016711	84.21
Ce-TiO_2	26.5	0.016711	84.32

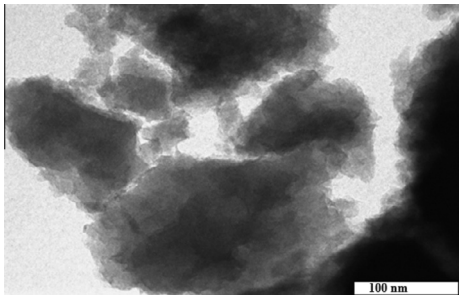

Fig. 6. TEM image of pure TiO_2.

The crystal violet dye solution at different pH values shows different colors and unstable. But at pH 6.5 it has remains in a blue violet color with an absorbance maximum at 590 nm, this is the natural color state of the crystal violet dye. Angeloni et al. [37] reported that at pH 1.0, the CV dye is yellow color with absorption maxima at 420 nm and 620 nm and CV gradually changes its color by increasing the acidity of the aqueous solution, being blue–green at pH 2–5. The different colors are a result of the different charged states of the dye molecule. In the yellow form, all three nitrogen atoms carry a positive charge, of which two are protonated. At neutral pH, both extra protons are lost to the solution, leaving only one of the nitrogen atoms positive charged [37]. In alkaline solutions, nucleophilic hydroxyl ions attack the electrophilic central carbon to produce the colorless triphenylmethanol or carbinol form of the dye. Suhail et al. [44] studied the effect of pH = 11 and pH = 12 on crystal violet dye but they did not consider this pH value because at pH = 11 turning color of crystal violet from violet to pale yellow, and this shows that the dye molecule structure is convert from case of saline formula to OH^- within pH = 11 therefore, the dyes is deposited at the bottom reaction vessel at this pH. The primary decolorization of synthetic waste water (crystal violet dye solution) in HC was performed by pumping of liquid solution through the cavitation device (circular venturi). Samples were taken for every 30 min over the time span of 90 min of experiment and analyzed for the UV absorbance for finding out the percentage decolorization of crystal violet dye in aqueous solution. Fig. 9 shows the extent of CV decolorization from the analysis of UV–Vis absorption spectra of crystal violet dye decolorization as a function of time. Concentration of CV decolorized in the presence of HC alone as a function of time was shown in the Fig. 10. It has been observed that crystal violet dye was decolorized up to ~45% when HC alone was alone used for 90 min.

The hydrodynamic characteristic of the cavitating device (circular Venturi) has been studied by measuring the flow rate in main line. The calculated CV for a circular venturi at an inlet pressure of 5 kg/cm^2 is 0.15 (CV = 0.15) according to the following equation [10,45]:

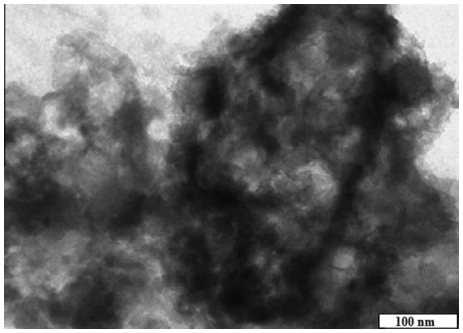

Fig. 7. TEM image of 1.6 mol% of Fe doped-TiO_2.

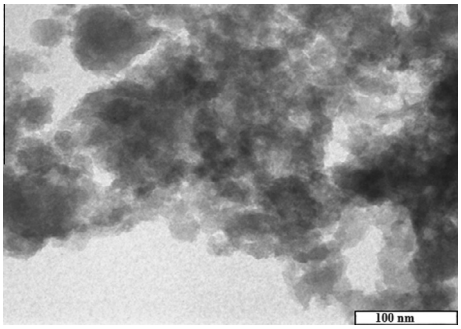

Fig. 8. TEM image of 1.6 mol% of Ce doped-TiO_2.

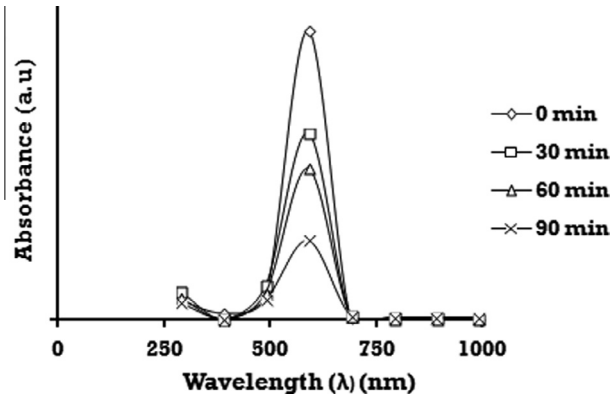

Fig. 9. Identification of CV decolorization from UV–Vis absorption spectra analysis [HC alone].

$$CV = \frac{P_2 - P_v}{\frac{1}{2}\rho v_0^2} \quad (2)$$

where

P_2 = fully recovered downstream pressure in kg/cm^2.
P_v = vapor pressure of the dye solution in kg/cm^2.
ρ = density of the dye solution in kg/m^{-3}.
v_0 = velocity of the dye solution at the throat of the cavitating constriction in m/s.

3.4. Effect of Fe–TiO_2 on CV decolorization

In a typical experimental study, UV photocatalysis has been coupled with hydrodynamic cavitation (HC) to make a hybrid advanced oxidation process (HAOP) for studying the synergy of the decolorization of crystal violet dye solution. In a typical hybrid AOP, 5 L of crystal violet dye solution consisting of 50 mg/L of dye and 0.6 g/L of 0.8% Fe–TiO_2 were used to study the decolorization rate of crystal violet dye at it's solution pH of 6.5. Samples were taken, filtered and tested using the UV spectrophotometry, after every 30 min interval in the total decolorization time of 90 min. similar procedure was followed for 1.6% of Fe–TiO_2 for finding out the decolorization rate of crystal violet dye following HAOP. It was observed that, 0.8% Fe–TiO_2 showed the extent of decolorization to 98%. Whereas 1.6% of Fe–TiO_2 showed the decolorization of 85% in 90 min of treatment.

Shirsath et al. [31] reported that, as doping content of iron on TiO_2 increased from 0.4 mol% to 1.2 mol%, the photocatalytic activity of the Fe doped TiO_2 increased but above 1.2 mol%, the photocatalytic activity of Fe doped TiO_2 decreased with an increase in the iron content. They also reported that small quantity of iron in TiO_2 is responsible for a reduction in the photo-generated hole–

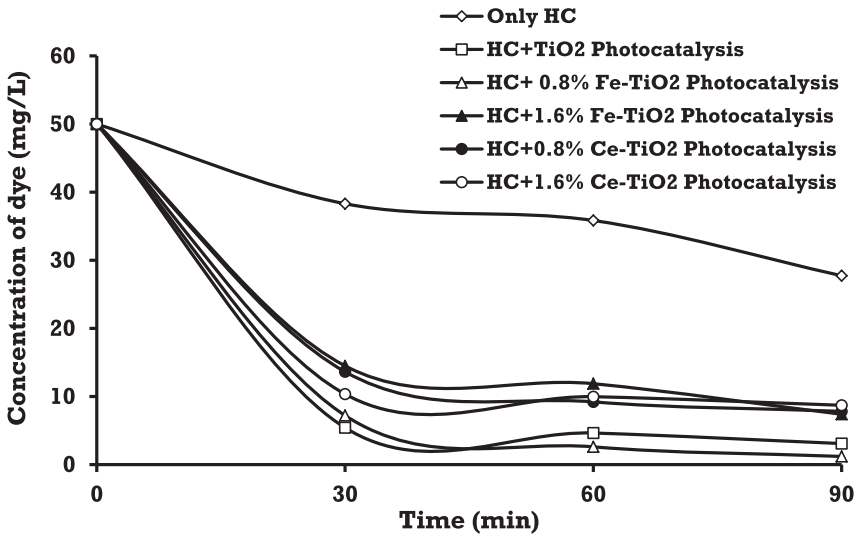

Fig. 10. Concentation of CV decolorized with respect to time [at pH = 6.5, inlet pressure = 5 bar, temperature = 35 °C, initial dye concentration 50 mg/L].

electron recombination rate. But at higher loadings, iron ions can serve as recombination centers and the photocatalytic activity of Fe doped TiO_2 decreases. This phenomenon is also demonstrated in some of the earlier investigations [2,6,24]. The results obtained with Fe doped TiO_2 and HC work was also matches with the results obtained by Shirsath et al. [31], in brief discussion, in this work doping has been carried out between 0 and 1.6 mol% i.e. doping with 0.8 and 1.6 mol% has been carried out. The doping of 0.8 mol% gives the maximum decolorization of 98%, whereas 1.6 mol% shows the reduction in decolorization. Doping with 1.6 mol% shown in reduction in decolorization has been reconfirmed from the results obtained by Shirsath et al. [31]. Thus, in this study 0.8 mol% iron doping on TiO_2 has been considered as the optimum doping concentration for the decolorization of crystal violet dye.

3.5. Effect of Ce–TiO_2 on CV decolorization

In this method, the prepared Ce–TiO_2 nanophotocatalyst with different doping percentages of 0.8% and 1.6% (Ce:TiO_2 mol%) was used for the decolorization studies of crystal violet dye. Each photocatalyst having 0.6 g/L of catalysts loading were tried for the decolorization studies. All the remaining parameters such as pH, dye concentration, volume of dye solution, temperature and pressure are kept constant throughout the process and were same as before. From the results, 0.8% Ce–TiO_2 showed the decolorization of ~84%. Whereas, 1.6% of Ce–TiO_2 showed the decolorization of ~82%. It was observed that the Ce doped TiO_2 did not show a significant effect on the degradation of crystal violet dye compared to the Fe doped TiO_2. It has been observed that crystal violet dye decoloration increased as the Ce content increased in the Ce-doped TiO_2 catalyst up to 1.0% i.e. 0.8% of Ce content. The increase in Ce loading may be attributed the photocatalytic activity of Ce doped TiO_2 by trapping of electrons in cerium sites with their subsequent transfer to the absorbed O_2 [30]. However, if the doping of Ce amount is continued to increase from 1.0% to 3.0%, then excess Ce dopant may introduce the indirect recombination of electrons and holes to reduce the photocatalytic activity, leading to a significant decrease in decolorization [25,30]. It has been observed that the degradation efficiency was higher when Ce content was below or equal to 1.0% in the TiO_2 catalyst and achieved 84% color removal after 90 min of treatment. While, the

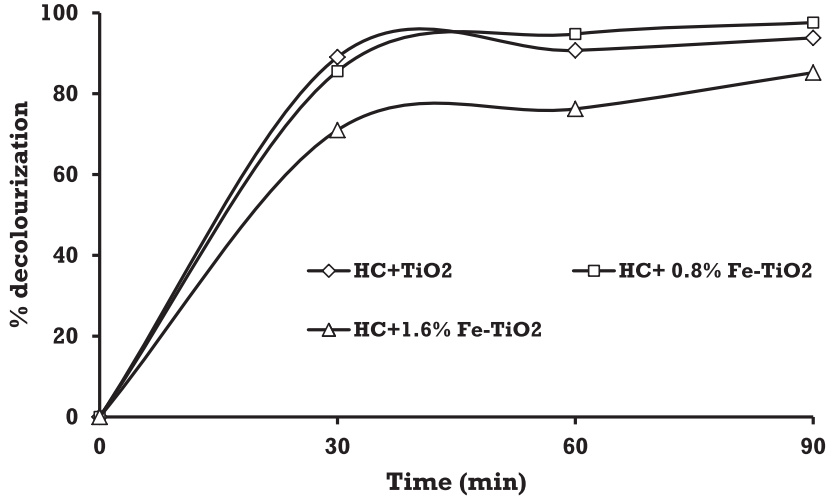

Fig. 11a. Percentage decolorization of CV dye in HC combined with pure TiO_2 and Fe doped TiO_2 [at pH = 6.5, inlet pressure = 5 bar, temperature = 35 °C, initial dye concentration 50 mg/L].

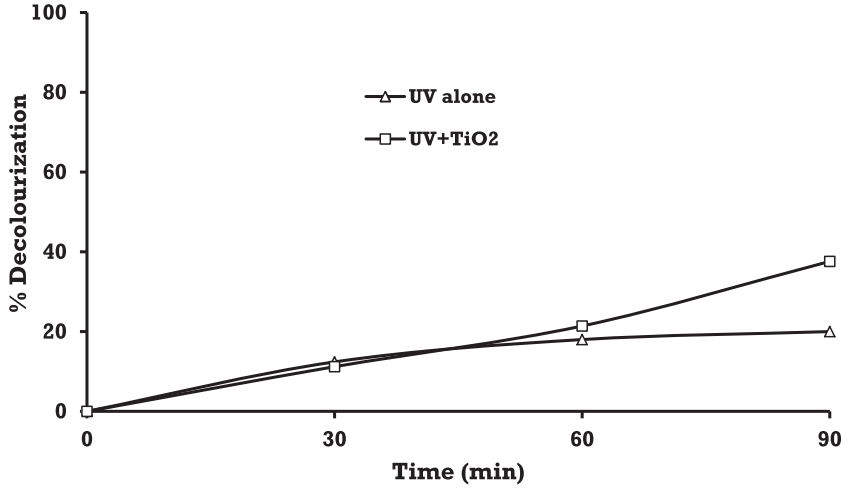

Fig. 11b. Percentage decolorization of CV dye in photolytic and photocatalytic processes [at pH = 6.5, inlet pressure = 5 bar, temperature = 35 °C, initial dye concentration 50 mg/L].

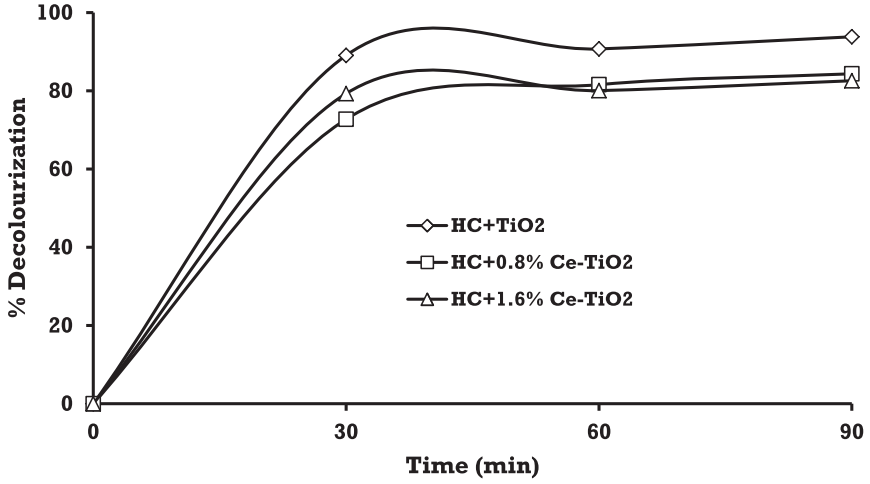

Fig. 11c. Percentage decolorization of CV dye in HC combined with Ce–TiO_2 [at pH = 6.5, inlet pressure = 5 bar, temperature = 35 °C, initial dye concentration 50 mg/L].

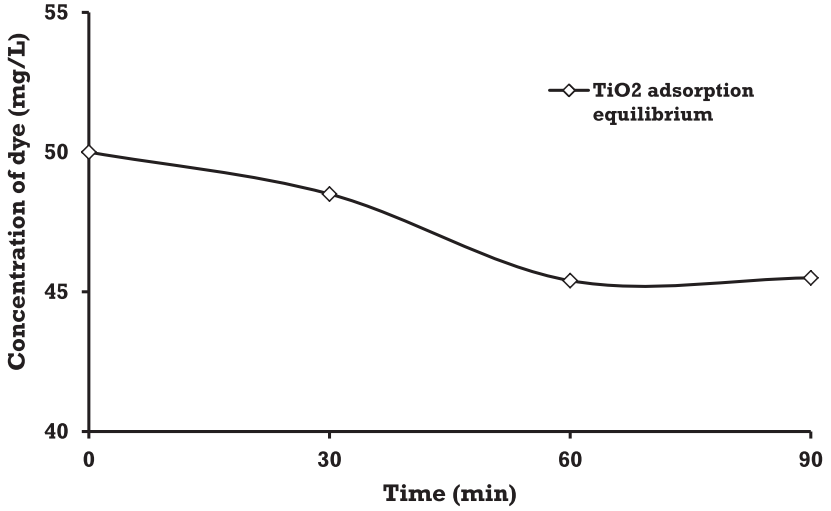

Fig. 12. Adsorption behavior of pure TiO_2 as a function of time.

decolorization efficiency was lower when Ce content was 1.6%, achieved 82% of color removal at the same time. This effect has been also observed in other reports [25, 30, and 31]. The results obtained in this work was also matches with the results obtained by the Ramirez et al. [33]. They have been studied the acid orange 7 (AO7) decolorization using Ce doped TiO_2 photocatalysts and reported lower photocatalytic activity for Ce doped TiO_2 than the pure TiO_2. Hence, in this study 0.8 mol% of Ce doping on TiO_2 has been considered as optimum loading concentration for decourization of crystal violet dye.

3.6. Effect of undoped TiO_2 on CV decolorization

To understand the effect of undoped TiO_2, 0.6 g/L of undoped TiO_2 were used for the decolorization of crystal violet dye at its normal pH (6.5) using HAOP. From the UV–Vis absorption spectra, it was observed that the crystal violet dye has been decolorized up to 94% when TiO_2 used along with HC. It has been observed that the undoped TiO_2 shown higher decolorization rate than 1.6% Fe–TiO_2, Ce–TiO_2 and 0.8% Ce–TiO_2. However shows less decolorization than 0.8% Fe–TiO_2. Graphical representation of percentage decolorization of CV dye in various systems was shown in the Fig. 11a–c.

3.7. Comparison of adsorption, photolytic, photo catalytic, HC+ photo catalytic processes

Initially, a study on adsorption equilibrium for TiO_2 surface has been established in 1 L of crystal violet dye solution. Further, we have evaluated the time required for achieving the adsorption equilibrium as well as the maximum amount of CV dye adsorbed onto the TiO_2 surface. This was attempted under agitation prior to carry out the actual experiments. Initially the crystal violet dye mixture was taken in a 1 L beaker and agitation was carried out with magnetic stirrer for 90 min in the dark environment to establish the equilibrium adsorption characteristics of undoped TiO_2. With the above procedure a maximum of 9% of crystal violet dye was adsorbed on to the TiO_2 (0.6 g/L loading) surface and adsorption equilibrium was obtained within 60 min of contact time. The equilibrium adsorption stage has been evaluated from the Fig. 12 contains a plot of concentration of CV dye Vs time. It has been observed from Fig. 12 the adsorption behavior of undoped TiO_2 after 60 min has shows no reduction in concentration of the CV dye with extended time of contact.

Table 2
Reaction rate constants (k) of CV degradation in different systems [at pH = 6.5, inlet pressure = 5 bar, temperature = 35 °C, initial dye concentration 50 mg/L].

Method	k Value (min^{-1})	Synergetic coefficient
UV alone	0.0029	–
UV + TiO_2	0.0048	–
HC	0.003	–
HC + TiO_2	0.0275	3.52
HC + TiO_2 + 0.8% Fe	0.0332	–
HC + TiO_2 + 1.6% Fe	0.017	–
HC + TiO_2 + 0.8% Ce	0.0289	–
HC + TiO_2 + 1.6% Ce	0.0302	–

Degradation of CV dye in photolytic process due to the generation of hydroxyl radicals by the dissociation of water molecules under UV irradiations. During the photolytic process, crystal violet dye decolorized up to 20%. Hence in photocatalytic process, the generation of hydroxyl radicals is more as compared to photolytic process, in this process, crystal violet dye has been decolorized up to 37.6%. It was observed that the maximum extent of decolorization of 94% was obtained using combined HC/UV + TiO_2 process, whereas, 44.5% and 37.6% of decolorization was obtained in HC and UV + TiO_2 alone respectively. The extent of decolorization in hybrid process has been attained due to generation of greater hydroxyl radical compared to individual operating processes (HC alone or UV + TiO_2 alone).

Synergetic effect of combined processes has been evaluated on the basis of reaction rate constant data of single and combined process. The synergetic index of the HC combined with TiO_2 photocatalysis has been calculated to evaluate the efficiency of the combined process of HC and TiO_2 photocatalysis to compare with individual process (HC and TiO_2 photocatalysis alone). The synergetic index (f) of HC combined with TiO_2 photocatalysis has been calculated by using the following equation shows synergetic effect of hybrid AOP:

$$f_{(HC+TiO_2\ \text{photocatalysis})} = \frac{k_{(HC+TiO_2\ \text{photocatalysis})}}{k_{(HC)} + k_{(TiO_2\ \text{photocatalysis})}} = \frac{0.0275}{0.003 + 0.0048} = 3.52 \quad (3)$$

3.8. Rate kinetics of CV decolorization

The degradation of organic pollutants in hydrodynamic cavitation will be occur by the generation of ·OH radicals and also

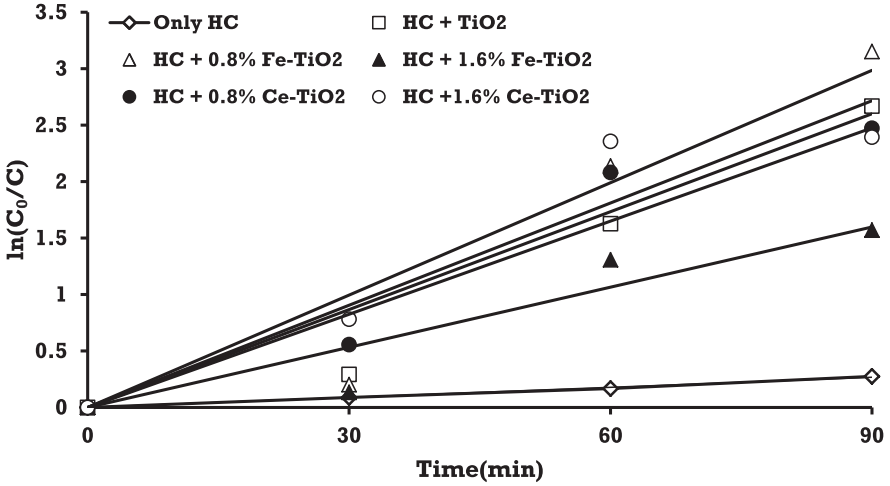

Fig. 13. Pseudo first order reaction kinetics of CV decolorization in HC and its combination with photocatalysis.

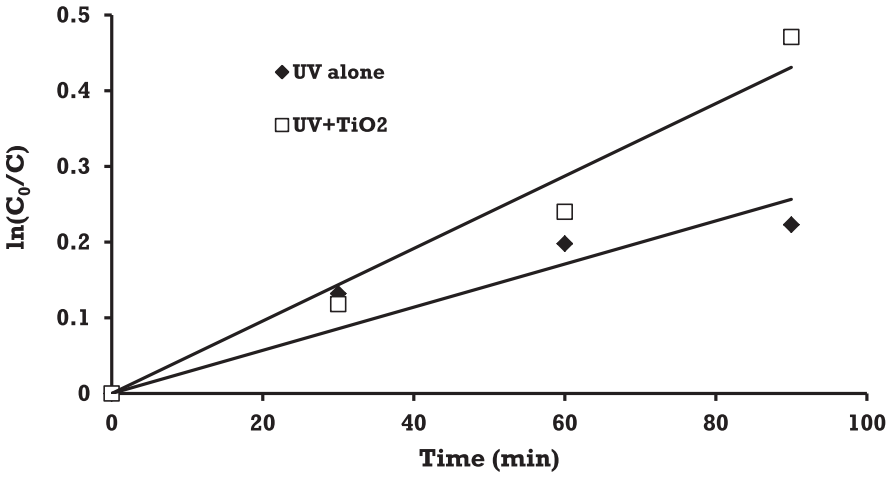

Fig. 14. Pseudo first order reaction kinetics of CV decolorization in photolytic and photocatalysis.

possibly due to the breakage of chromophore. These ·OH radicals are rapidly react with CV dye, which is present at the interface of the cavities and the waste water. Most of the investigators reported that the degradation reactions of many organic pollutants in advanced oxidation processes followed a pseudo first order reaction. The rate constants of degradation reaction of CV dye has been calculated using the following equation:

$$\ln\left(\frac{C_0}{C}\right) = k \times t \tag{4}$$

where '*C*' is the concentration of dye molecules present in mol/L, '*k*' is the rate constant in min^{-1} and '*t*' is the time in minutes.

The kinetic mechanism for decolorization of CV dye using hydrodynamic cavitation coupled with photocatalysis followed a first order reaction as confirmed by the plot of $\ln(\frac{C_0}{C})$ vs. time (t). The plot of $\ln(\frac{C_0}{C})$ vs. time (t) is a straight line and it passes through the origin. Reaction rate constants (k) of CV decolorization in different systems (HC alone and HC + photocatalysis) has been reported in Table 2. Pseudo reaction kinetics of CV decolorization in various systems was shown in the Figs. 13 and 14.

4. Conclusion

From this work, it has been concluded that, a novel synthesis technique was successfully implemented for the production of undoped and doped TiO_2 nanophotocatalysts. Photocatalysts prepared by sonochemical technique has shown good and uniform doping on TiO_2 and confirms the crystalline nature, when it is calcined at 200 °C. Approximately half of the CV dye in aqueous solution has been decolorized when the HC is used alone. Whereas, further decolorization has been achieved when hybrid technique (HC + photocatalysis) was used. In the hybrid technique, 0.8% Fe-doped TiO_2 photocatalyst has shown the maximum decolorization about 98% than other photocatalysts such as Ce-TiO_2 and pure TiO_2.

Acknowledgment

Shirish H. Sonawane acknowledges the Ministry of Environment and Forest (MoEF, Govt of India) for providing the financial support thorough Grant No.: 10-1/2010-CT (WM).

References

[1] Y. Anjaneyulu, N. Sreedhara Chary, D. Samuel Suman Raj, Decolourization of industrial effluents available methods and emerging technologies a review, Rev. Environ. Sci. Biotechnol. 4 (2005) 245–273.
[2] U.G. Akpan, B.H. Hameed, Parameters affecting the photocatalytic degradation of dyes using TiO_2-based photocatalysts: a review, J. Hazard. Mater. 170 (2009) 520–529.
[3] G.L. Baughman, E.J. Weber, Transformation of dyes and related compounds in anoxic sediments: kinetics and products, Environ. Sci. Technol. 28 (1994) 267–276.
[4] S. Papic, D. Vujevic, N. Koprivanac, D.S. Inko, Decolorisation and mineralization of commercial reactive dyes by using homogeneous and heterogeneous Fenton and UV/Fenton processes, J. Hazard. Mater. 164 (2009) 1137–1145.
[5] M.S. Lucas, J.A. Peres, Decolorization of the azo dye reactive Black 5 by Fenton and photo-Fenton oxidation, Dyes Pigm. 71 (2006) 236–244.
[6] S. Velazquez-Peña, C. Sáez, P. Cañizares, I. Linares-Hernández, V. Martínez-Miranda, C. Barrera-Díaz, M.A. Rodrigo, Production of oxidants via electrolysis of carbonate solutions with conductive-diamond anodes, Chem. Eng. J. 230 (2013) 272–278.
[7] Y.G. Adewuyi, Sonochemistry in environmental remediation. 2. Heterogeneous sonophotocatalytic oxidation processes for the treatment of pollutants in water, Environ. Sci. Technol. 39 (2005) 8557–8570.
[8] J. Chen, M. Liu, J. Zhang, X. Ying, L. Jin, Photocatalytic degradation of organic wastes by electrochemically assisted TiO_2 photocatalytic system, J. Environ. Manage. 70 (2004) 43–47.
[9] F. Parolin, U.M. Nascimento, E.B. Azevedo, Microwave-enhanced UV/H_2O_2 degradation of an azo dye (tartrazine): optimization, colour removal, mineralization and ecotoxicity, Environ. Technol. 34 (2013) 1247–1253.
[10] K.M. Kalumuck, G.L. Chahine, The use of cavitating jets to oxidize organic compounds in water, J. Fluids Eng. Trans. ASME 122 (2000) 465–470.
[11] X. Wang, J. Wang, P. Guo, W. Guo, C. Wang, Degradation of Rhodamine B in aqueous solution by using swirling jet-induced cavitation combined with H_2O_2, J. Hazard. Mater. 169 (2009) 486–491.
[12] X. Wang, J. Jia, Y. Wang, Electrochemical degradation of reactive dye in the presence of water jet cavitation, Ultrason. Sonochem. 17 (2010) 515–520.
[13] K.S. Suslick, M.M. Mdleleni, J.T. Ries, Chemistry induced by hydrodynamic cavitation, J. Am. Chem. Soc. 119 (1997) 9303–9304.
[14] P.R. Gogate, A.B. Pandit, Engineering design methods for cavitation reactors II: hydrodynamic cavitation, AIChE J. 46 (2000) 1641–1649.
[15] M. Zhou, J. Yu, B. Cheng, Effects of Fe-doping on the photocatalytic activity of mesoporous TiO_2 powders prepared by an ultrasonic method, J. Hazard. Mater. B137 (2006) 1838–1847.
[16] H. Wang, J. Niu, X. Long, Y. He, Sonophotocatalytic degradation of methyl orange by nano-sized Ag/TiO_2 particles in aqueous solutions, Ultrason. Sonochem. 15 (2008) 386–392.
[17] Y. Li, S. Peng, F. Jiang, G. Lu, S. Li, Effect of doping TiO_2 with alkaline-earth metal ions on its photocatalytic activity, J. Serb. Chem. Soc. 72 (2007) 393–402.
[18] U.G. Akpan, B.H. Hameed, Enhancement of the photocatalytic activity of TiO_2 by doping it with calcium ions, J. Colloid Interface Sci. 357 (2011) 168–178.
[19] Y.H. Peng, G.F. Huang, W.Q. Huang, Visible-light absorption and photocatalytic activity of Cr-doped TiO_2 nanocrystal films, Adv. Powder Technol. 23 (2010) 8–12.
[20] M.A. Barakat, H. Schaeffer, G. Hayes, S. Ismat-Shaha, Photocatalytic degradation of 2-chlorophenol by Co-doped TiO_2 nanoparticles, Appl. Catal. B: Environ. 57 (2004) 23–30.
[21] A.M.T. Silva, C.G. Silva, G. Drazic, J.L. Faria, Ce-doped TiO_2 for photocatalytic degradation of chlorophenol, Catal. Today 144 (2009) 13–18.

[22] M.A. Rauf, M.A. Meetani, S. Hisaindee, An overview on the photocatalytic degradation of azo dyes in the presence of TiO_2 doped with selective transition metals, Desalination 276 (2011) 13–27.
[23] K. Koci, K. Mateju, L. Obalova, S. Krejcikova, Z. Lacny, D. Placha, L. Capek, A. Hospodkova, O. Solcov, Effect of silver doping on the TiO_2 for photocatalytic reduction of CO_2, Appl. Catal. B: Environ. 96 (2010) 239–244.
[24] Y. Li, C. Xie, S. Peng, G. Lu, S. Li, Eosin Y-sensitized nitrogen-doped TiO_2 for efficient visible light photocatalytic hydrogen evolution, J. Mol. Catal. A: Chem. 282 (2008) 117–123.
[25] M. Asilturk, F. Sayılkan, E. Arpac, Effect of Fe^{3+} ion doping to TiO_2 on the photocatalytic degradation of Malachite Green dye under UV and visirradiation, J. Photochem. Photobiol. A: Chem. 203 (2009) 64–71.
[26] H.K. Shon, D.L. Cho, S.H. Na, J.B. Kim, H.J. Park, J.H. Kim, Development of a novel method to prepare Fe- and Al-doped TiO_2 from wastewater, J. Ind. Eng. Chem. 15 (2009) 476–482.
[27] S. Chang, W. Liu, Surface doping is more beneficial than bulk doping to the photocatalytic activity of vanadium-doped TiO_2, Appl. Catal. B: Environ. 101 (2011) 333–342.
[28] N. Venkatachalam, M. Palanichamy, B. Arabindoo, V. Murugesan, Enhanced photocatalytic degradation of 4-chlorophenol by Zr^{4+} doped nano TiO_2, J. Mol. Catal. A: Chem. 266 (2007) 158–165.
[29] Z.L. Shi, C. Du, S.H. Yao, Preparation and photocatalytic activity of cerium doped anatase titanium dioxide coated magnetite composite, J. Taiwan Inst. Chem. Eng. 42 (2011) 652–657.
[30] J. Wang, Y. Lv, L. Zhang, B. Liu, R. Jiang, G. Han, R. Xu, X. Zhang, Sonocatalytic degradation of organic dyes and comparison of catalytic activities of CeO_2/TiO_2, SnO_2/TiO_2 and ZrO_2/TiO_2 composites under ultrasonic irradiation, Ultrason. Sonochem. 17 (2010) 642–648.
[31] S.R. Shirsath, D.V. Pinjari, P.R. Gogate, S.H. Sonawane, A.B. Pandit, Ultrasound assisted synthesis of doped TiO_2 nano-particles: characterization and comparison of effectiveness for photocatalytic oxidation of dyestuff effluent, Ultrason. Sonochem. 20 (2013) 277–286.
[32] R.L. Narayana, M. Matheswaran, A.A. Aziz, P. Saravanan, Photocatalytic decolourization of basic green dye by pure and Fe, Co doped TiO_2 under daylight illumination, Desalination 269 (2011) 249–253.
[33] R.J. Ramirez, J.V. Sanchez, S.S. Martinez, Solar assisted degradation of acid orange 7 textile dye in aqueous solutions by Ce-doped TiO_2, Mex. J. Sci. Res. 1 (2012) 42–55.
[34] L. Andronic, D. Andrasi, A. Enesca, M. Visa, A. Duta, The influence of titanium dioxide phase composition on dyes photocatalysis, J. Sol–Gel. Sci. Technol. 58 (2011) 201–208.
[35] S. Samira, P. Akash Raja, C. Mohan, J.M. Modak, Photocatalytic degradation of crystal violet (C.I. basic violet 3) on nano TiO_2 containing anatase and rutile phases (3:1), J. Thermodyn. Catal. 3 (2012).
[36] M. Sivakumar, A.B. Pandit, Wastewater treatment: a novel energy efficient hydrodynamic cavitational technique, Ultrason. Sonochem. 9 (2002) 123–131.
[37] L. Angeloni, G. Smulevich, M.P. Marzocchi, Resonance Raman spectrum of crystal violet, J. Raman Spectrosc. 8 (1979) 305–310.
[38] X. Wang, J. Jia, Y. Wang, Degradation of C.I. reactive red 2 through photocatalysis coupled with water jet cavitation, J. Hazard. Mater. 185 (2011) 315–321.
[39] M.V. Bagal, P.R. Gogate, Degradation of diclofenac sodium using combined processes based on hydrodynamic cavitation and heterogeneous photocatalysis, Ultrason. Sonochem. 21 (2014) 1035–1043.
[40] I.H. Perez, A.M. Maubert, L. Rendón, P. Santiago, H.H. Hernández, L. Díaz Arceo, V. Garibay Febles, E.P. González, L. González-Reyes, Ultrasonic synthesis: structural, optical and electrical correlation of TiO_2 nanoparticles, Int. J. Electrochem. Sci. 7 (2012) 8832–8847.
[41] H.K. Shon, S. Vigneswaran, J. Kandasamy, M.H. Zareie, J.B. Kim, D.L. Cho, J.H. Kim, Preparation and characterization of titanium dioxide (TiO_2) from sludge produced by $TiCl_4$ flocculation with $FeCl_3$, $Al_2(SO_4)_3$ and $Ca(OH)_2$ coagulant aids in wastewater, Sep. Sci. Technol. 44 (2009) 1525–1543.
[42] Y. Xie, C. Yuan, Visible-light responsive cerium ion modified titania sol and nanocrystallites for X-3B dye photodegradation, Appl. Catal. B: Environ. 46 (2003) 251–259.
[43] S.T. Hayle, G.G. Gonfa, Synthesis and characterization of titanium oxide nanomaterials using sol–gel method, Am. J. Nanosci. Nanotechnol. 2 (2014) 1–7.
[44] F.S.A. Suhail, M.S. Mashkour, D. Saeb, The study on photo degradation of crystal violet by polarographic technique, Int. J. Basic Appl. Sci. 15 (2015) 12–21.
[45] P. Senthil Kumar, M. Siva Kumar, A.B. Pandit, Experimental quantification of chemical effects of hydrodynamic cavitation, Chem. Eng. Sci. 55 (2000) 1633–1639.